32ND INTERNATIONAL COSMIC RAY CONFERENCE, BEIJING 2011

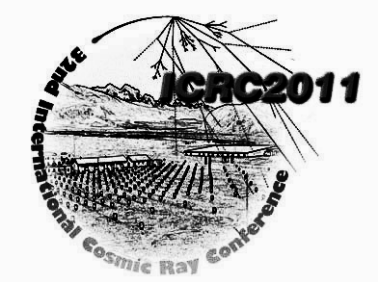

The cloud monitor by an infrared camera

F. SHIBATA[1], K. HONDA[1], T. TOMIDA[1], Y. TSUNESADA[2], H. TOKUNO[2], M. FUKUSHIMA[3], M. CHIKAWA[4], FOR THE TELESCOPE ARRAY COLLABORATION
[1]*University of Yamanashi, Interdisciplinary Graduate School of Medicine and Engineering, Kofu, Yamanashi*
[2]*Tokyo Institute of Technology, Meguro, Tokyo, Japan*
[3]*Institute for Cosmic Ray Research, University of Tokyo, kashiwa, Chiba, Japan*
[4]*Kinki University, Higashi Osaka, Osaka, Japan*

g10mh011@yamanashi.ac.jp

Abstract: The mesurement of the extensive air shower using the fluorescence detectors (FDs) is affected by the condition of the atmosphere. In particular, FD aperture is limited by cloudiness. If cloud exists on the light path from extensive air shower to FDs, fluorescence photons will be absorbed drastically. Therefore cloudiness of FD 's field of view (FOV) is one of important quality cut condition in FD analysis. In the Telescope Array (TA), an infrared (IR) camera with a filed of view of $25.8^\circ \times 19.5^\circ$ has been installed at an observation site for cloud monitoring during FD observations. This IR camera measures temperature of the sky every 30 min during FD observation. Clouds can be seen at a higher temperature than areas of cloudless sky from these temperature maps. In this paper, we discuss the quality of the cloud monitoring data, the analysis method, and current quality cut condition of cloudiness in FD analysis.

Keywords: UHECRs, cloud monitoring, Atomspheric minitoring, Infra-red, Infra-red camera

1 Introduction

In the Telescope Array (TA) experiment we have started hybrid observations with both surface detector array (SD) and fluorescense detector (FD) in the Utah desert to study origin of ultra high energy cosmic rays (UHECRs) with enegies greater than 10^{18} eV since May 2008. The fluorecence detectors are installed in the three observation sites. 12 detectors at "Black Rock Mesa (BR)" and "Long Ridge (LR)" stations, and 14 detectors at "Middle Drum (MD)" station are located. The surface detector array (SD) consists of 512 scintillation detectors in the area of 700 km^2 at 1.2 km interval. For analysis fluorescence data, atmospheric monitoring is a very important factor, because the propagation process of fluorescence photons are scattered and absorbed by aerosols, molecules, or clouds in the atomsphere. Therefore, we have introduced a LIDAR system, the Central Laser Facility (CLF), and an infra-red (IR) camera as the atmosphere monitoring system. The LIDAR system measures the back-scattering light of the laser to obtain the atmospheric transparency. The CLF is located at the center of FD stations. FDs observe the side scattering light of the laser shooted vertically from CLF for measuring an atmospheric transparency. The IR camera measures the existence of the cloud by measuring infrared rays. We describe the cloud monitoring system using the IR camera in this paper.

2 The Cloud Monitoring System

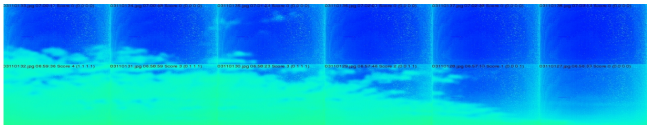

Figure 1: The sky above Black Rock Mesa station seen by the IR camera: two elevation angles 10.5° and 25.5°, and 6 azimathal directions for each elevation

The IR camera (Avio-TVS 600) is installed at Black Rock Mesa station for the cloud monitoring system, and started data acquisition from December 2007. As specification of this IR camera, it can measure sensitive in a wavelength range of $8 \sim 14$ [μm], in temperature range of $-20 \sim 300$ [°C]. This IR camera measures sky temperature in a FOV of $25.8^\circ \times 19.5^\circ$ (slightly larger than that of FD) and digitizes in 320×236 pixels for one image. The IR camera is mounted on steering table that be changed in elevation and azimuthal directions via PC control. In an observation sequence, 14 IR images are taken every half hour, 12 IR images for the directions of the FDs in the station (two elevation angles 10.5° and 25.5°, and 6 azimuthal directions for each elevation), and the horizontal and the vertical directions. The time required to take one IR image including

a direction change is $\sim$ 30 second, it takes about 7 minutes for an observation sequence. For the cloud monitoring during a day, IR data acquirable by observation of one night is 60 $\sim$ 150 IR images depending on seasonal observation times, and the data sizes mount to 10 $\sim$ 25 MB. An example of the "sky map" is shown in Fig.1. We can see clearly the condition of cloud from this example.

3 Analysis (Identifying Clouds)

3.1 Pixel Data Distribution

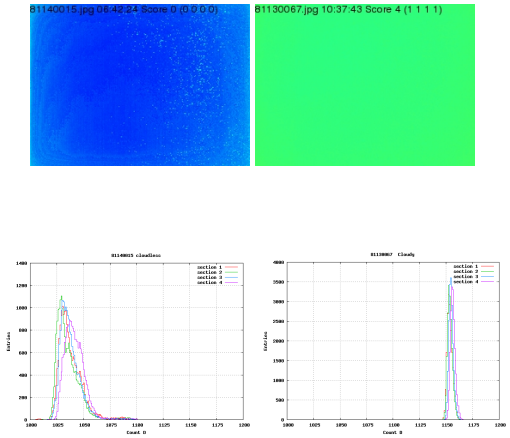

Figure 2: Example of IR images and distributions of the pixel count D of cloudless and cloudy skies (for lower elevation angle, 10.5°).

Examples of IR images of cloudless and cloudy skies in upper elevation angle (25.5°), and the distributions of pixel count D are shown Fig.2. The pixel count D = 1100 corresponds to temperature ~ -20[°C], and D = 1200 for $\sim$ 0[°C]. We divide an IR image into four "sections" (320 $\times$ 59 pixels) considering elevation dependence of sky temperature, and we cull "section" 1, 2, 3, and 4 from the top. Figure 2 can be seen that clouds are measured higher temperature, conversely cloudless sky are measured lower temperature. Since the IR images of the section 3 and 4 in lower elevation angle (10.5°) always are measured higher temperature to near the ground, IR images of that are identify the cloudy by mistake. Therefore, we don't use to score of section 3 and 4 for "identifying clouds".

3.2 Identifying Clouds

In order to evaluate cloud coverage in an IR image, we employ a statistical analysis method. First, we classify every IR images into cloudless or cloudy skies by checking eyes, however, the image that mixes with cloudy and cloudless is not put in this sort. (The data separated by eye-selected is named "training data") Second, we define the median of the pixel count D with each section in one IR images by using "training data". (The median of the pixel

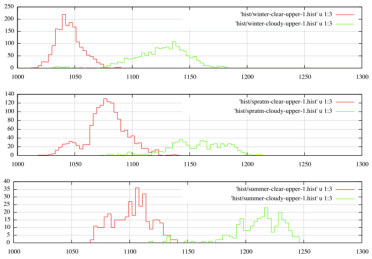

Figure 3: The ditribution of D_{50} for eye-selected cloudless and cloudy skies :above figure (winter) and center figure(spring-fall), and below figure (summer)

count D is named "D_{50}") Since D_{50} is shifted by seasonal dependences, after IR images is splited by eye-selected. We divide into the three groups of summer (July-Augast) and winter (December-April), and spring-fall (May-June, September-October). Figure 3 shows distributions of D_{50} for eye-selected cloudless (red line) and cloudy (green line) skies for 3 seasonal groups. If there is a cloud, the pixel distributioin shifts right and D_{50} is larger than one of cloudless sky. It can be seen that for each of the four sections the distributions D_{50} of the cloudless and the cloudy skies in seasonal groups are splited. Then we analyze by different classification on D_{50} of an IR image for each of the sections and the lower and the upper elevations (10.5° and 25.5°), and three seasonal groups (summer and winter, and spring-fall). Here "the cloud probability" is used for the distribution D_{50} according to Baye's theorem ,such that

$$p(Cloudy \mid D_{50}) = \frac{p(D_{50} \mid Cloudy)\, p(Cloudy)}{p(D_{50})} \tag{1}$$

$$p(Cloudy) = \frac{Cloudy\ training\ data}{Total\ training\ data} \tag{2}$$

$$p(D_{50}) = p(D_{50} \mid Clear)\, p(Clear) + p(D_{50} \mid Cloudy)\, p(Cloudy) \tag{3}$$

We judge cloudy events which p(Cloudy | D_{50}) is larger than 50%. If p(Cloudy | D_{50}) for a section is larger than 50%, the section is flagged "1" (Cloudy), otherwise "0" (Clear). By summing the 0/1 flags of the four sections, we define a score of an IR image from 0 to 4. For example, the IR image on the left of Fig.2 is the probability of (0.02,0.01,0.02,0.04), accordingly it is scored as 0 = (0,0,0,0). And the IR image on the right of Fig.2 is the probability of (1.00,1.00,1.00,1.00), accordingly it is scored as 4 = (1,1,1,1). The IR images for eye-selected cloudless and cloudy are correctly judged score "0" (cloudless) or "4" (cloudy) by "the cloud probability". "The cloud probability" for the four sections are determined for the lower and the upper elevation angles, and the seasonal groups independently.

3.3 The entire evaluation

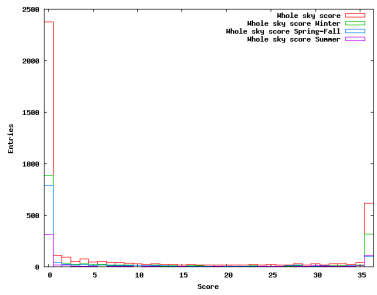

Figure 4: Distribution of total score of the IR images for 12 directions

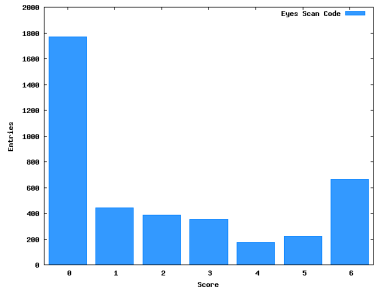

Figure 5: Distribution of score of the Eyes-scan Code

We carried out the analysis of the IR data obtained from 2007/Dec/29 ∼ 2010/10/16, ∼ 40000 IR images. The distribution of total score, a sum of the scores of the 12 directions above the Black Rock Mesa station is shown in Fig.4. There are peaks at scores 0 and 36. This suggests that if there is a cloud in one direction in the FOV of the IR camera, most of the sky seen from the station is covered with clouds. The clasic cloud monitor is Eyes-scan method from old time. Eyes-scan Code is checked existence of the cloud by the eyes. As same as IR camera analysis, the section if flagged "1" (Cloudy), or "0" (Clear). We divide the sky roughly into six sections for Eyes-scan, North, South, West, East, zenith, and near horizontal area looking from Black Rock Mesa. We difine the socres of Eyes-scan Code from 0 to 6 summing the 0/1 flags of the six sections. The distribution of total scores in Eyes-scan Code is shown in Fig.5. As shown Fig.4 and Fig.5, the scores of IR camera consists with that of Eyes-scan Code.

4 Analysis (The cloud height calculation)

4.1 The cloud height with an IR camera

The height is calculated from IR images and it is compared with the height of CLF and LIDAR. If we know the correct height with an IR camera, there may be practicable data even by the data judged to cloudy by an analysis of above mention. For example, when the cloud of low height existed in the FD's FOV, fluorescence photons will be absorbed drastically. When the cloud of high height existed in the FD's FOV, fluorescence photons is not absorbed because an air shower phenomenon occurs after passing the cloud. Here, We perform the analysis with the vertical IR images.

4.2 Cloud height calculation method

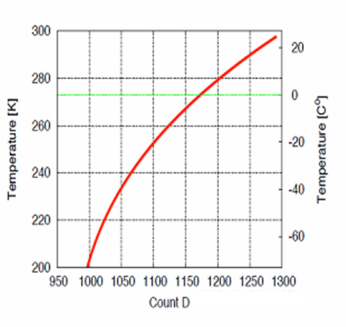

Figure 6: Correlation chart with temperature and pixel count D

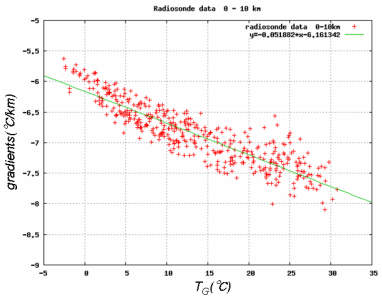

Figure 7: The correlation of The gradients and temperature in 0 km of the radiosonde

We carried out the analyze of the IR data obtained about 1200 IR images. The cloud height is calculated by

$$Height = \frac{T_{IR} - T_G}{\gamma} \quad (4)$$

Here, empty temperature assumes it T_{IR}, ground temperature T_G, temperature lapse rate γ. Firstly we calculate empty temperature Temp (T_{IR}). D_{50} of the area which is the center (80 ∼ 240 pixels, 59 ∼ 177 pixels) of the IR image is used. D50 is converted into temperature from Fig. 6. Figure 6 is temperature and a correlation chart of pixel count D. Next, the ground temperature (T_G) uses a value acquired with an IR camera. Finally, we calculate temperature lapse rate (γ). The temperature lapse rate uses the data of the radiosonde. The radiosonde is an apparatus to observe weather data (temperature, the humidity, atmospheric

pressure) from the ground to the sky. Data of a radiosonde uses data for two years in seven vicinities of experimental place. In the range of 0 $\sim$ 10km to be given by the data of the radiosonde, we calculate in the least-squares method of the linear functions. The correlation of The gradients and temperature in 0 km of the radiosonde is Fig.7. A function found with a least square from figure 7 is

$$\gamma = -0.052T_G - 6.16 \quad (5)$$

And the temperature of the ground of IR camera is substituted for the system (5). The height of clouds with the IR image is found when we substitute these for the system (4).

4.3 Height comparison with CLF, LIDAR

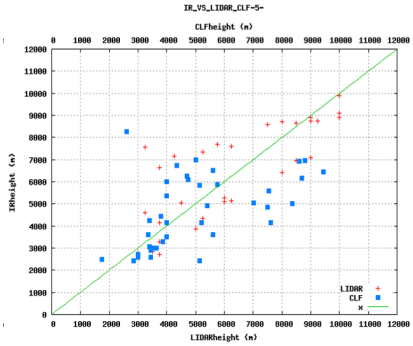

Figure 8: Height scatter plot of LIDAR, CLF and the IR

The height of IR camera compare with the height found with CLF, LIDAR. And because an atmospheric scattering becomes the peak level, the height is calculated as the cloud. And the data of CLF and IR are used only for difference less than one hour in the same date. Even as for the data of LIDAR and the IR likewise. The result was narrowed down to 38 cases in IR and CLF, 30 examples in IR and LIDAR. Figure 8 is scatter plot of the each height. If a straight line of Fig.8 includes a point, the height is the same. There is also the point far greatly, but the data of IR and CLF, LIDAR are relatively consistent.

5 Result

From our analysis, The total score "0", that is, the cloudless is judged to be entire 58% and the score "36", that is, the cloudy is entire 15% as shown in Fig.4. Similarly in Eyes-scan Code, The score "0", that is, the cloudless is judged to be entire 44% and the score "6", that is, the cloudy is entire 16% as shown in Fig.5. Without being judged that there is a partly cloud, IR camera tends to be judged to be the whole cloudless or cloudy than Eyes-scan Code. Even numeric statistics in IR camera and Eyes-scan Code, the scores of IR camera almost consists with that of Eyes-scan Code. The IR camera can be searched for existance of clouds automatically unlike Eyes scan, and the total scores obtained from the IR data is useful to the data selection of fluorescence events. When cloud height is compared IR with CLF, LIDAR, it is the same height relatively. But it'll be necessary to increase in future because statistics are few. For the analysis of the first stage, We used the data of the vertical of FOV, The cloud height is being analyzed by data of elevation angles 10.5° and 25.5°.

6 Conclusion

The cloud monitoring system using the IR camera for TA experiment has been running quite stably since 2007/Dec/29. We use analysis method to judge existence of clouds by defining the score of IR images divided the pixel data into four sections and the threshold as 50% of "the cloud probability". In order to reduce the seasonal dependence of temperature, we divide into diffrent thresholds for data of summer and winter and, spring-fall. The IR camara analysis method consists with Eyes-scan method. We can see the existence of clouds automatically with the IR camera, and the IR camara score is useful to FD data selection. When cloud height is compared IR with CLF, LIDAR, it is the same height relatively. We used the data of the vertical of FOV, The cloud height is being analyzed by data of elevation angles 10.5° and 25.5°.

7 Acknowledgement

The Telescope Array experment is supported by the Ministry of Education, Culture, Sports, Science and Technology-Japan through Kakenhi grants on priority area "Highest Energy Cosmic Rays"; by the U.S National Science Foundation awards; by the Korean Science and Engineering Foundation; by the Russian Academy of Sciences. The State of Utah supported the project through its Economic Development Board, and the University of Utah through the Office of the Vice President for Research.The experimental site became available through the cooperation of the Utah School and Institutional Trust Lands Asministration (SITLA), U.S Bureau of Land Management and the U.S. Air Force. We also wish to thank the people and officials of Millard Country, Utah, for their steadfast and warm support. We gratefully acknowledge the contributions from the technical staffs of our home institutions.

References

[1] Cosmic ray astrophysics,(1972)
[2] The First Observation with the Fluorescence Detectors of the Telescope Array Experiment, 30^{th} ICRC Proc.,(2007)
[3] Ovservation of ultra high energy cosmic rays with the surface detector array of the TA experiment, 30^{th} ICRC Proc.,(2007)
[4] Cloud Monitoring with Infra-Red camera for the Telescope Array Experiment, 31^{st} ICRC Proc.,(2009)